Original Research Article

Ganoderma lucidum Polysaccharides Prevent Platelet-Derived Growth Factor-Stimulated Smooth Muscle Cell Proliferation *in vitro* and Neointimal Hyperplasia in the Endothelial-Denuded Artery *in vivo*

SHU-HUEI WANG,[1] CHAN-JUNG LIANG,[1] YU-WEN WENG,[1] YUNG-HSIANG CHEN,[2] HSIEN-YEH HSU,[3] HSIUNG-FEI CHIEN,[4] JAW-SHIUN TSAI,[5] YING-CHIN TSENG,[6] CHI-YUAN LI,[7*] YUH-LIEN CHEN[1*]

[1]Department of Anatomy and Cell Biology, College of Medicine, National Taiwan University, Taipei
[2]Institute of Clinical Medical Science, China Medical University, Taichung
[3]Institute of Biotechnology in Medicine, National Yang-Ming University, Taipei
[4]Department of Surgery, National Taiwan University Hospital, National Taiwan University, Taipei
[5]Department of Family Medicine, National Taiwan University Hospital, National Taiwan University, Taipei
[6]Department of Obstetrics and Gynecology, Hsinchu Cathay General Hospital, Hsinchu
[7]Graduate Institute of Clinical Medical Science, China medical university, Taichung, Taiwan

The first three authors contributed equally to this study.

***Correspondence to:** Dr. Yuh-Lien Chen, Department of Anatomy and Cell Biology, College of Medicine, National Taiwan University, No. 1, Section 1, Ren-Ai Rd, Taipei, 100, Taiwan. Telephone: +886-2-23123456-88176, Fax: +886-2-33931713, E-mail: ylchenv@ntu.edu.tw; Dr. Chi-Yuan Li, Graduate Institute of Clinical Medical Science, China medical university, No.91 Hsueh-Shih Road, Taichung, Taiwan. Telephone: + 886-4-22052121-3562, Fax: +886-4-22052121-3598, E-mail: cyli168@gmail.com.

Running head: EORP PREVENTS VSMC PROLIFERATION
Contract grant sponsor: National Science Council and the Cooperative Research Program of the NTU and CMUCM, Taiwan, Republic of China.
Contract grant number: NSC 99-2320-B-002-022-MY3 and 100F008-404

Additional Supporting Information may be found in the online version of this article.

Received 10 March 2011; Revised 23 September 2011; Accepted 28 September 2011
Journal of Cellular Physiology

DOI 10.1002/jcp.23053

ABSTRACT

Ganoderma lucidum is used in traditional Chinese medicine to prevent or treat a variety of diseases, including cardiovascular disorders. We previously demonstrated that a glucan-containing extract of Reishi polysaccharides (EORP) has the potent anti-inflammatory action of reducing ICAM-1 expression in lipopolysaccharide (LPS)-treated human aortic endothelial cells (HASMCs) and LPS-treated mice. In the present study, we examined whether EORP inhibited platelet-derived growth factor-BB (PDGF)-stimulated HASMC proliferation and the mechanism involved. EORP dose-dependently reduced cell numbers and DNA synthesis of PDGF-treated HASMCs *in vitro*. EORP also arrested cell cycle progression in the G0/G1 phase, and this was associated with decreased expression of cyclin D1, cyclin E, CDK2, CDK4, and $p21^{Cip1}$ and upregulation of the cyclin-dependent kinase inhibitor $p27^{Kip1}$. The antiproliferative effect of EORP was partly mediated by downregulation of PDGF-induced JNK phosphorylation. In *in vivo* studies, the femoral artery of C57BL/6 mice was endothelial-denuded and the mice were fed a diet containing 100 mg/Kg/day of EORP. On day 14, both cell proliferation (proliferating cell nuclear antigen-positive cells) in the neointima and the neointima/media area ratio (0.67±0.03 versus 1.46±0.30) were significantly reduced. Our data show that EORP interferes with the mitogenic activation of JNK, preventing entry of HASMCs into the cell cycle *in vitro* and reducing cell proliferation in the neointima and decreasing the neointimal area *in vivo*. Thus, EORP may represent a safe and effective novel approach to the prevention and treatment of vascular proliferative diseases.

Keywords: Reishi / smooth muscle cells / cell cycle / proliferation / restenosis

Introduction

The abnormal accumulation of smooth muscle cells (SMCs) in the arterial intima is an important event in the development of atherosclerosis, postangioplasty/in-stent restenosis, transplant vasculopathy, and vessel bypass graft failure (Dzau et al., 2002; Ross, 1995). The identification of the key mechanisms involved in SMC function will help in understanding cellular responses to vascular injury. The above pathological conditions are characterized, to varying degrees, by proliferation of SMCs that have migrated from the media to form the neointima. In addition, elevated platelet-derived growth factor (PDGF) levels are one of the most important risk factors for atherosclerosis and cardiovascular morbidity (Heldin and Westermark, 1999). SMC proliferation, triggered by increased PDGF levels, is a prominent feature of the complex pathobiology and the identification of novel compounds with combined anti-inflammatory and antiproliferative properties may improve existing therapeutic strategies by limiting late cardiovascular complications, such as in-stent restenosis or bypass graft failure (Andres and Castro, 2003).

The fungus *Ganoderma lucidum* (*G. lucidum*, Reishi), a famous home remedy, has long been known for its beneficial effects on human health and longevity and its ability to cure various human diseases, such as hepatitis, hypertension, hyperglycemia, and cancers (Shiao, 2003; Wang et al., 2002). Polysaccharides isolated from *G. lucidum* have been shown to be the bioactive constituents responsible for its various health benefits, such as its antioxidant, anti-cancer, anti-inflammatory,

and immunomodulatory activities (Gao et al., 2005; Miyazaki and Nishijima, 1981; Sun et al., 2004; Wang et al., 1997). We have previously demonstrated that a glucan-containing extract of Reishi polysaccharides (EORP) attenuates ICAM-1 expression and monocyte adherence of LPS-treated human aortic smooth muscle cells (HASMCs) and that this protective effect appears critical in preventing the development of vascular inflammation and disease (Lin et al., 2010). Recently, the effects of *G. lucidum* extracts on cancer, which is characterized by cell proliferation, have been widely studied. *G. lucidum* polysaccharides have been shown to exhibit antitumor activity and reduce tumor metastasis (Gao et al., 2005) and a *G. lucidum* extract has been shown to inhibit the proliferation of human prostate cancer cells (Evans et al., 2009), SW480 human colorectal cancer cells (Xie et al., 2006), and breast cancer cells (Jiang et al., 2004; Jiang et al., 2006) and to have anticancer effects against the HL-60 and U937 leukemic cell lines (Wang et al., 1997). However, it is unclear whether EORP, in addition to having antiinflammatory properties, has a direct effect on cell cycle progression and the proliferation of vascular SMCs and thus might even prevent highly proliferative vascular responses, such as postangioplasty restenosis. Cell cycle progression is regulated by cell cycle regulator proteins and these are, in turn, regulated by mitogen-activated protein kinases (MAPKs) and the PI3-K/Akt signaling pathway (Zhan et al., 2003). We were therefore interested in examining the action of EORP on human aortic smooth muscle cells (HASMCs) stimulated by PDGF-BB and whether it affected the expression of cell cycle-related proteins, an important event in cell proliferation. In addition, we examined its effects on intimal thickening and cell proliferation in a mouse model of vascular injury. Our results showed that

EORP attenuated cell proliferation both *in vitro* and *in vivo* and that inhibition of JNK phosphorylation may be a key mechanism involved in the antiproliferative effect of EORP.

Materials and methods

Preparation of EORP

The biologically active compounds from *G. lucidum*, identified as the fucose-containing glycoprotein fraction and named extract of Reishi polysaccharides (EORP), were isolated as described previously (Hsu et al., 2004; Wang et al., 2002). A crude powder of *G. lucidum*, prepared by alkaline extraction with 0.1 N NaOH, followed by neutralization and ethanol precipitation, was obtained from Pharmanex (Provo, UT). The crude powder (6 g) was dissolved in 120 mL of double-distilled water, stirred at 4 °C for 12 h, and centrifuged at 250 g for 1 h at 4ºC to remove insoluble material. The resulting solution was concentrated at 40-50 °C to a small volume and lyophilized to generate 5 g of dark brown powder. This water-soluble residue was stored at –20 °C until used for further purification. Briefly, a 2.1 g sample was dissolved in a small volume of 0.1 M Tris buffer, pH 7.0, containing 0.1% sodium azide and purified by gel filtration chromatography at 4 °C using a Sephacryl S-500 column (95 x 2.6 cm) with 0.1 M Tris buffer, pH 7.0, as eluent at a flow rate of 0.6 mL/min and collecting 6.0 mL per tube. Each fraction was subjected to carbohydrate detection with phenol-H_2SO_4, then five fractions (fractions 1–5) were pooled, concentrated at 40-50

°C to a small volume, dialyzed to remove salts and sodium azide, and lyophilized to give 520 mg (25%) of EORP.

HASMC cultures

HASMCs, purchased as cryopreserved tertiary cultures from Cascade Biologics (OR, USA), were grown in culture flasks in smooth muscle cell growth medium (M231, Cascade Biologics Inc.) supplemented with 5% smooth muscle growth supplement, penicillin (100 units/mL), streptomycin (100 pg/mL), and Fungizone (1.25 μg/mL) at 37 °C in a humidified 5% CO_2 atmosphere. The growth medium was changed every other day until confluence, then the cells were passaged every 3-5 days and used between passages 3 and 8. All cells were synchronized in serum-free medium for 24 h prior to experiments. For all data shown, the experiments were repeated at least 3 times in duplicate with different preparations of HASMCs. For Western blot analysis, the graphical analysis represents the results from three independent experiments and quantification by densitometry.

Effect of PDGF and EORP on cell viability

To evaluate the effect of EORP on HASMC proliferation, which contributes to vascular lesion formation (Ross, 1995), HASMCs were plated at a density of 10^4 cells/well in 96-well plates, then, after overnight growth, were treated with different concentrations of PDGF-BB or EORP, then cell viability was measured using the 3-(4,5-dimethylthiazol-2-yl)-2,5-diphenyltetrazolium bromide (MTT) assay. In brief, MTT (0.5 mg/mL) was applied to the cells for 4 h to allow the conversion of

MTT into formazan crystals, then, after washing with phosphate-buffered saline (PBS), the cells were lysed with dimethyl sulfoxide and the absorbance read at 550 nm on an ELISA reader. The optical density after drug treatment was used as a measure of cell viability and was normalized to that of cells incubated in control medium, which were considered 100% viable.

BrdU incorporation into HASMCs

HASMCs were seeded on pre-coated coverslips at a concentration of $5x10^4$ cells in serum free-M231 medium for 24 h in the absence or presence of different concentrations of EORP. After overnight growth, the cells were treated with different concentrations of PDGF and 5-bromo-2'-deoxy-uridine (BrdU) labeling reagent using a kit from Sigma. The labeling reagent was added to the medium at a final concentration of 30 μM and the cells incubated for 24 h, then the culture medium was removed and 100 μL of fixative solution added for 30 min at room temperature (RT). The fixative was then removed and the cells washed with 3 x 100 μL of PBS, then 100 μL of mouse anti-BrdU antibody was added for 30 min at 37ºC. The anti-BrdU antibody solution was then removed and the cells rinsed with 3 x 100 μL of PBS, then rhodamine-conjugated goat anti-mouse IgG antibody (1:200, Eappel) was added for 30 min at RT. After immunostaining, BrdU-immunoreactive cells from six visual fields under 20x objective in each culture, and DAPI (1 μg/mL)-stained cells, representing the total cell number were counted. The overall percentage of proliferative cells for each group was expressed as a mean of these six values. All experiments were performed at least three times.

Effect of PDGF and EORP on cell death

Cell death was quantified using the lactate dehydrogenase (LDH) assay, based on the measurement of LDH activity released from the cytosol of dying cells into the supernatant. The culture supernatants were collected and were determined by MaxDiscovery Lactate Dehydrogenase Cytotoxicity assay kit as manufacture's protocol (Bioo Scientific Corp, Austin, USA).

Terminal deoxynucleotide transferase dUTP Nick End Labeling (TUNEL) assay

The TUNEL technique was used to detect DNA fragmentation of the cells in situ according to the instructions provided by the manufacturer (TdT-FragEL^{TM}, DNA fragmentation detection kit, CALBIOCHEM, MA). Briefly, adherent cultured cells were fixed in 4% paraformaldehyde for 15 min at RT, and endogenous peroxidase was quenched with 3 % H_2O_2 for 5 min. The sections were incubated with terminal deoxynucleotidyl transferase (TdT) and a mixture of biotin-labeled nucleotides for 90 min. This was followed by incubation with anti-streptavidine-peroxidase for 30 min and color development with H_2O_2-diaminobenzidine. Then, the slides were counterstained with methyl green. For positive controls (PC), cells treated with 1 µg/µL DNaseI (in 1X TBS/1mM $MgSO_4$) at RT for 20 min.

Cell cycle analysis

Analysis of the DNA content and the movement of the cells through the mitotic cycle was performed by flow cytometry 24 h after cell stimulation. HASMCs were harvested, fixed in 80%

ethanol, and stored in a −20 °C freezer for 30 min, then were washed twice with ice-cold PBS and incubated with 10 μL of RNAase (20 μg/mL, Qiagen, Germany) and 50 μL of propidium iodide (20 μg/mL, Sigma). Cell cycle phase analysis was performed by flow cytometry using a FACScan (Becton Dickinson, USA), and the percentage of cells in different phases of the cell cycle analyzed using ModFitLT software.

Preparation of cell lysates and Western blot analysis

To prepare cell lysates, the cells were lysed for 1 h at 4ºC in 20 mM Tris-HCl, 150 mM NaCl, 1 mM EDTA, 1 mM EGTA, 1 % Triton X-100, 1 mM phenylmethylsulfonyl fluoride, pH 7.4, then the lysate was centrifuged at 4000 *g* for 30 min at 4ºC and the supernatant retained. Western blot analyses were performed as described previously (Lin et al., 2005). Briefly, samples of cell lysate (20 μg of protein) were subjected to 12% SDS-PAGE and transferred to PVDF membranes, which were then treated with 3% nonfat milk in 0.1 M phosphate buffer for 1 h at RT to block nonspecific binding of antibody. The membranes were then incubated with rabbit antibodies against human phospho-Akt, human phospho-JNK, human total JNK, human total ERK1/2, human cyclin D1, or human $p27^{kip1}$ or mouse antibodies against human phospho-ERK1/2, human cyclin E, or human CDK4 (all from Cell Signaling, USA), goat antibodies against human total p38 or rabbit antibodies against human phospho-p38 (Santa Cruz, USA), or rabbit antibodies against human CDK2 or human $p21^{Cip1}$ (Gene Tex, USA), all at a dilution of 1:1000, then with horseradish peroxidase-conjugated goat anti-rabbit or goat anti-mouse or rabbit anti-goat IgG antibodies

(1:3000, Sigma), bound antibodies being detected using Chemiluminescence Reagent Plus (NEN, MA, USA). The intensity of each band was quantified using a densitometer. Antibodies against β-actin (Sigma), α-tubulin (Millipore, USA), or GAPDH (1:1000, Santa Cruz) were used as loading controls.

Knockdown of gene expression using small interfering RNA

Knockdown of JNK gene expression was performed by transfection with small interfering RNA (siRNA). Cells (5×10^6) were resuspended in 100 μL of nucleofector solution (Amaxa Biosystems, Germany), and gene-specific siRNA oligomers (1 μM) were electroporated according to the manufacture's instruction manual. The JNK siRNAs (Catalog # 10620319 124945 G01 and 10620318 124945 G02) were AUC UGA AUC ACU UGC AAA GAU UUG and CAA AUC UUU GCC AAG UGA UUC AGA U. Cells were transfected for 48 h. The siRNA results were evaluated by Western blotting.

Mouse femoral arterial injury model and immunohistochemical staining

Male 8-week-old C57BL6 mice (n=24), weighing between 25 and 35 g, were purchased from the National Taiwan University (Taipei, Taiwan). For all surgical procedures, the mice were anesthetized by intraperitoneal (i.p.) injection of 30-40 mg/kg of pentobarbital diluted in 0.9% sodium chloride solution. All procedures involving experimental animals were performed in accordance with the guidelines for animal care of the National Taiwan University and complied with the "Guide for the Care and Use of Laboratory Animals" NIH publication No. 86-23, revised 1985. Trans-luminal mechanical injury of the left femoral artery was induced basically according to

the method developed by Sata *et al*. (Sata et al., 2000). Briefly, the artery was exposed by blunted dissection and was looped proximally and distally with 6-0 silk suture for temporary vascular control during the procedure. A small branch between the rectus femoris and vastus medialis muscles was isolated and looped proximally and ligated distally with 6-0 silk sutures. The muscular branch artery was exposed by transverse arteriotomy and dilated by topical application of one drop of 1% lidocaine hydrochloride. Microsurgery forceps were used to extend the arterioctomy, through which a straight spring wire (0.38 mm in diameter, No. C-SF-15-15, COOK, Bloomington, IN, USA) was carefully inserted into the femoral artery for more than 5 mm towards the iliac artery. The wire was left in place for 1 min to denude and dilate the artery, then was removed, and the silk suture looped at the proximal portion of the muscular branch artery secured. Blood flow in the femoral artery was restored by releasing the sutures placed in the proximal and distal femoral portions and the skin incision was closed with a 6-0 silk suture. To examine the effects of EORP administration on neointimal formation in the endothelial-denuded femoral artery, the mice were divided into 2 groups. The treatment period was 2 weeks (days 0-14), with D1 being the day of endothelial denudation. Groups 1 and 2 were given, respectively, PBS or oral EORP at 100 mg/Kg/day on days 0-14. At the end of treatment, the mice were euthanized by i.p. injection of an overdose of sodium pentobarbital and the left femoral artery gently dissected, rinsed with ice-cold PBS, immersion-fixed in 4% buffered paraformaldehyde, OCT-embedded, and cross-sectioned for morphometric analysis and immunohistochemistry. The 5 mm long femoral artery was cut serially into 8 μm frozen sections and every tenth section was stained with Resorcin-Fuchsin solution

(Sigma).

For morphometric analysis of neointimal formation, the mean neointima/media cross-sectional area (I/M) ratio for 10-15 sections per animal was calculated using Image-Pro Plus 4.5 and the equation: I/M area ratio= [internal elastic lamina (IEL) area- lumen area]/[external elastic lamina area-IEL area]. Cell proliferation was assessed by looking for actively cycling cells within the neointima by incubation of sections overnight at 4ºC with anti-mouse PCNA monoclonal IgG (1:100 dilution, Santa Cruz, CA), rinsing with PBS, and incubation with a prediluted biotin-conjugated anti-mouse IgG antibodies (Vector) for 1 h at RT, followed by washing with PBS. Bound antibody was detected by incubation for 1 h at RT with avidin-biotin-horseradish peroxidase complex (Vector), followed by 0.5 mg/mL of 3,3'-diaminobenzidine/0.01% hydrogen peroxide in 0.1 M Tris-HCl buffer, pH 7.2, as chromogen (Vector Lab, USA). Negative controls were performed by omitting the primary antibody. The results were analyzed under a microscope and positive staining for PCNA quantified as the number of cells staining brown in the total number of cells in six different fields of vision for every sample and expressed as the PCNA-positive cells/total cells ratio. The average ratio for the six different fields was taken as the PCNA-positive index. To detect smooth muscle cells, the serial section was incubated with mouse anti-α-actin (1:25, Dako) and then incubated for 1 h at RT in a 1:200 dilution of FITC conjugated goat anti-mouse IgG antibody (Sigma).

Statistical analysis

All data were expressed as the mean ± S.E.M. The difference in mean values among different

groups was analyzed by one-way ANOVA and a subsequent post hoc Dunnett test. A value of $P < 0.05$ was considered statistically significant.

Results

Cell viability was assessed using the MTT assay. After 48 h incubation with 1, 2.5, 5, or 10 μg/mL of EORP, cell viability was, respectively, 1.08± 0.06, 0.95 ± 0.06, 0.91± 0.04, or 0.92± 0.06 of control levels (data not shown), showing that EORP treatment did not result in cytotoxicity. After 24 h incubation with 10, 20, 30, or 40 ng/mL of PDGF, cell viability was, respectively, 1.18±0.15, 1.23±0.04, 1.50±0.04, or 1.49±0.11 of control levels (data not shown), showing that the two highest concentration causing a significant increase in cell viability. To determine whether EORP affected PDGF-induced cell proliferation, cells were pretreated with 1, 2.5, 5, or 10 μg/mL EORP for 24 h, then stimulated with 30 ng/mL of PDGF for 24 h and tested by the MTT assay, trypan blue exclusion, and Brd U incorporation. HASMCs incubated with 30 ng/mL of PDGF showed a significant increase in cell viability (Fig 1A), cell number (Fig. 1B), and BrdU uptake (Figs. 1C and D) compared to controls. EORP had a concentration-dependent inhibitory effect on PDGF-induced cell proliferation (Figs. 1B and D), the effect being significant at 5 or 10 μg/mL EORP. In addition, the effect of EORP on the decrease of cell proliferation in PDGF-treated HASMCs was not caused by cytotoxicity examined by LDH assay (Fig. 1E) and cell apoptosis by TUNEL assay (Fig. 1F).

Flow cytometric analysis was then used to determine whether the EORP-induced cell growth inhibition was due to arrest at a specific point of the cell cycle. As shown in Table 1, flow cytometric analysis of the DNA content of HASMCs showed that treatment for 24 h with 30 ng/mL of PDGF alone caused a significant increase in the percentage of cells in S phase (from 2.0 ± 0.3% to 5.5± 0.7%) and in G2/M phase (from 8.9 ± 0.6% to 13.0 ± 0.8%) and a significant decrease in the G0/G1 populations (from 89.2 ± 0.5% to 81.6 ± 1.2%) relative to control cultures. Pretreatment of HASMCs with 10 μg/mL of EORP followed by PDGF treatment resulted, respectively, in a significant reduction compared to PDGF treatment alone in the percentage of cells in S phase (from 5.5± 0.7% to 3.5± 0.6%) and in the percentage of cells in the G2/M population (from 13.0 ± 0.8% to 10.6 ± 0.6%), accompanied by a significant accumulation of cells in G0/G1 phase (from 81.6 ± 1.2% to 86.0 ± 0.9%). These data show that EORP inhibits DNA synthesis in PDGF-treated HASMCs by inhibiting the cell transition from G0/G1 to S phase of the cell cycle.

Uncontrolled cellular proliferation is the result of cell cycle disorganization and deregulation of specific cellular processes that control cell cycle progression and checkpoint reservation through the intermitotic phases. These events are highly regulated by cyclins and cyclin-dependent kinases (CDKs) (Golias et al., 2004; Kim et al., 2004). Since the above data showed that EORP treatment induced cell-cycle arrest at G0/G1, we investigated the mechanism involved. HASMCs with or without EORP pretreatment before PDGF stimulation were analyzed

for the expression of different components of the cyclin-dependent complexes that are important in regulating cell cycle progression. As shown in Fig. 2, 30 ng/mL of PDGF alone caused a marked increase in the expression of cyclin D1 (Fig. 2A), CDK4 (Fig. 2B), cyclin E (Fig. 2C), and CDK2 (Fig. 2D), and these effects were significantly reduced with 5 or 10 μg/mL EORP. We also assessed the effect on the expression of $p27^{Kip1}$ and $p21^{Cip1}$, two cyclin-dependent kinase inhibitors (CDKIs) that are known to regulate the entry of the cells into S phase (Golias et al., 2004). $p27^{Kip1}$ expression was reduced to 22±1% of control levels after 24 h exposure to PDGF and this effect was inhibited by EORP (Fig. 2E). In contrast, PDGF caused a significant increase in $p21^{Cip1}$ protein levels which was inhibited by EORP treatment in a concentration-dependent manner (Fig. 2F).

Since cell proliferation caused by exposure to growth factors is linked to activation of MAPKs and Akt (Zhan et al., 2003), we examined whether PDGF-stimulated cell proliferation in HASMCs was associated with activation of MAPKs and Akt. As shown in Fig. 3, phosphorylation of JNK (Fig. 3A), p38 (Fig. 3B), ERK (Fig. 3C), and Akt (Fig. 3D) was significantly increased at 15 and 30 min after PDGF addition. Interestingly, EORP pretreatment significantly attenuated the JNK and p38 phosphorylation induced by PDGF treatment for 30 min, but had no effect on ERK and Akt phosphorylation (Figs. 3A-3D). Inactivation or attenuation of JNK signaling can be accomplished by dephosphorylation of JNKs by a growing family of dual specificity phosphatases, including MAPK phosphatase-1 (MKP-1) (Desbois-Mouthon et al.,

2000). We observed that MKP-1 expression was significantly increased after 30 min of EORP treatment (Fig. 3E), corresponding to the time of EORP-induced JNK inhibition (Fig. 3A).

To further determine whether the anti-proliferative effect of EORP was mediated by inactivation of the MAPK pathway, the effect of EORP on DNA synthesis was examined by Brd U incorporation after treatment of HASMCs for 6 h with 30 μM SP600125 (a JNK inhibitor), SB203580 (a p38 inhibitor), or PD98059 (an ERK inhibitor). As shown in Fig. 4A and 4B, SP600125, SB203580, or PD98059 significantly inhibited PDGF-induced BrdU incorporation. Moreover, EORP also had an additive effect on BrdU incorporation when compared with SB203580 or with PD98059 treatment alone. In contrast, EORP and SP600125 co-treatment or SP600125 alone had a significant and similar inhibitory effect on PDGF-induced HASMC proliferation. These results suggest that inhibition of JNK phosphorylation is a key mechanism in the antiproliferative effect of EORP. The JNK pathway may be the essential trigger for early cell cycle events. We found that the JNK inhibitor SP600125 alone reduced PDGF-induced expression of CDK4 (Fig. 5B), cyclin E (Fig. 5C), CDK2 (Fig. 5D) and $p21^{Cip1}$ (Fig. 5F). p38 inhibitor SB203580 and ERK inhibitor PD98059 significantly inhibited PDGF-induced cyclin E and $p21^{Cip1}$ expression and cyclin E, CDK2 and $p21^{Cip1}$ expression, respectively. The PDGF-induced cyclin D1 expression (Fig. 5A) and PDGF-reduced $p27^{Kip1}$ expression (Fig. 5E) was not affected by all of three inhibitors. HASMCs transfected with JNK-specific siRNA significantly inhibited the expression of CDK4 (Fig. 6B), cyclin E (Fig. 6C), CDK2 (Fig. 6D) and

$p21^{Cip1}$ (Fig. 6F), not cyclin D1 (Fig. 6A) and $p27^{Kip1}$ (Fig. 6E). The effectiveness of the siRNA caused a 60 % reduction in JNK protein expression (Fig. 6G).

To examine the effects of EORP administration on neointimal formation in the endothelial-denuded femoral artery model, mice were divided into 2 groups. The treatment period was 2 weeks (days 0-14), with D1 being the day of endothelial denudation and one group received oral EORP administration at 100 mg/Kg/day on days 0-14, while the other group did not. Over the experimental period, there was no difference in weight gain and final weight between the two groups. Morphometric analysis showed that the intima/media area ratio in the EORP-treated endothelial-denuded artery of mice (0.67±0.03, n = 12) was significantly lower than that in the endothelial-denuded mice (1.46±0.30, n=12) (Figs. 7A, 7B). To study the effect of EORP on cell proliferation in endothelial-denuded mice, immunohistochemical staining with antibodies against PCNA or anti-α actin antibody (staining smooth muscle cells) was carried out on serial sections. As shown in Figs 7C and 7D, in the endothelial-denuded mice, PCNA-positive cells were seen on the thickened intima of the femoral artery (Figs. 7C, 7D), while, in the EORP-treated endothelial-denuded artery, the intimal area was reduced and showed significantly fewer PCNA-positive cells. Some PCNA-positive cells were labeled by anti-smooth muscle cell antibody in serial section. In addition, EORP treatment showed weaker ICAM-1 expression in the intimal area (Fig. 7E).

Discussion

In the present study, we showed that EORP treatment attenuated the proliferation of PDGF-stimulated HASMCs *in vitro* and cell proliferation in the endothelial-denuded artery of mice *in vivo*. EORP treatment of PDGF-stimulated HASMCs induced arrest of cell cycle progression, downregulation of expression of cyclin D1, cyclin E, CDK2, and CDK4, and upregulation of expression of the CDK inhibitor $p27^{Kip1}$. The antiproliferative effect of EORP might therefore be mediated by regulation of JNK phosphorylation.

Reishi extract was chosen for testing, as it has long been known as a health food and is used in traditional oriental medicines as an anti-inflammatory, anti-tumor, antioxidant, and immunomodulatory agent (Gao et al., 2005; Miyazaki and Nishijima, 1981; Wang et al., 1997; Wang et al., 2002). Some studies have shown that Reishi extracts prevent the proliferation and invasiveness of some kinds of cancer cells and macrophages (Dudhgaonkar et al., 2009; Evans et al., 2009; Sliva et al., 2002; Thyagarajan et al., 2006; Wang et al., 2009). These include the finding that *G. lucidum* extract inhibits the proliferation of human breast cancer cells by downregulation of estrogen receptor and NF-κB signaling (Jiang et al., 2006). G. lucidum extract also attenuates the PDGF-activated proliferation of hepatic stellate cells by blocking the PDGF receptor (Wang et al., 2009). The present study demonstrated that EORP inhibited the PDGF-induced proliferation of HASMCs and this effect was not caused by cytotoxicity and cell apoptosis.

As revealed by the flow cytometric assay, the antiproliferative effect of EORP was associated with an accumulation of cells in G0/G1 phase of the cell cycle. Whereas PDGF-stimulated cells transitioned into S phase, EORP blocked PDGF-induced cell cycle progression. This is in accordance with a previous report that a *G. lucidum* extract induces G0/G1 cell-cycle arrest in human breast cancer cells and that this is closely correlated with decreased cell proliferation (Jiang et al., 2004). These results show that EORP targets signaling transduction events at G0/G1-S interphase. Cell cycle control is a highly regulated process that involves a complex cascade of events. Modulation of the expression and function of the cell cycle regulatory proteins (including cyclins, CDKs, and CDKIs) provides an important mechanism for inhibition of growth (Golias et al., 2004). Here, we showed that, in the presence of EORP, downregulation of cyclin D1, cyclin E, CDK4, and CDK2 expression in PDGF-treated cells occurred in parallel with decreased DNA synthesis, cell growth inhibition, and decreased entry into S phase. These observations suggest that the antiproliferative activity of EORP in PDGF-treated HASMCs involves a multifaceted attack on multiple target molecules critically involved in growth inhibition.

The activity of the cyclin/CDK complex is affected by the action of the CDKIs $p21^{Cip1}$ and $p27^{kip1}$. CDKIs, can bind tightly to, and inhibit the kinase activity of, several cyclin-CDK complexes, such as cyclin D1-CDK4 and cyclin E-CDK2, and arrest cell growth at the G1 and G1/S boundary, and thus function in growth regulation (Golias et al., 2004). Consistent with the view, our data showed that PDGF downregulated $p27^{Kip1}$ and this effect was reversed by EORP. Although the

decrease in $p21^{Cip1}$ expression is regulated through the cell cycle machinery, there is evidence that the increase in $p21^{Cip1}$ may affect cell proliferation by maintaining cyclin/CDK complex function (Ghosh et al., 2003; Shankland and Wolf, 2000). In our study, PDGF induced expression of $p21^{Cip1}$ and this was blocked by EORP. Increased $p21^{Cip1}$ expression is observed during proliferation because it acts a scaffold to facilitate the assembly of cyclins and CDKs required for DNA synthesis (Ghosh et al., 2003; Shankland and Wolf, 2000). In spite of the fact that $p21^{Cip1}$ was originally identified as an inhibitor, it may act as an adaptor protein (Moon et al., 2004). Thus, the loss of CDK kinase components, including cyclin D1, cyclin E, CDK4, and CDK2, the downregulation of $p21^{Cip1}$, and the upregulation of $p27^{Kip1}$ caused by EORP treatment may be a downstream mechanism by which EORP exerts its antiproliferative effect on PDGF-treated HASMCs. To our knowledge, this is the first study showing the involvement of each component of the CDKI-cyclin-CDK machinery during the cell-cycle arrest of vascular SMCs induced by EORP.

MAPKs and Akt are involved in PDGF-induced vascular SMC proliferation (Zhan et al., 2003). Our study showed that PDGF caused strong activation of three MAPK subtypes and Akt in HASMCs, as reported in rat aortic SMCs in a previous study (Ishizawa et al., 2009). However, whether their activation is involved in the protective mechanism of EORP remains unclear. EORP treatment significantly attenuated the PDGF-induced phosphorylation of JNK and p38, but had no effect on ERK and Akt phosphorylation. Furthermore, although the commonly used blockers of the MAPK pathway that we tested (SP600125, a JNK inhibitor; SB203580, a p38 inhibitor;

PD98059, an ERK inhibitor) reduced the proliferative effects of PDGF. EORP treatment had no additional effect to SP600125 alone on PDGF-induced proliferation, as shown by BrdU incorporation, but did have an additive effect when compared with SB203580 or PD98059 treatment alone. On the basis of the above findings, it is likely that the role of JNK in the effects of EORP on the inhibition of PDGF-induced cell proliferation appeared to be greater than those of p38 and ERK. In the present study, we also demonstrated that decreased activation of the JNK pathway resulted in insufficient expression of the cell cycle proteins (CDK4, cyclin E, CDK2, and $p21^{Cip1}$) that control the G0/G1/S phase progression of HASMCs, resulting in inhibition of proliferation. Although several studies have shown that Reishi extracts prevent the proliferation and invasiveness of some kinds of cancer cells and macrophages mediated by MAPKs or by the Akt pathway (Dudhgaonkar et al., 2009; Jiang et al., 2004; Wang et al., 2009), to our knowledge, this is the first study showing that inhibition of JNK phosphorylation may be a key mechanism of the anti-proliferative effect of EORP in PDGF-treated HASMCs.

SMC accumulation in the arterial intima is a key event in the pathogenesis of many vascular diseases and is characterized by the de-differentiation, migration, and proliferation of medial-derived SMC to form the neointima (Ross, 1995). A proliferating cell population and coordinated augmentation of PDGF expression are seen in the neointima of the severely injured artery and this is followed by a drastic increase in neointimal cross-sectional area (Uchida et al., 1996), suggesting that the cellular proliferation stimulated by PDGF contributes to neointimal

growth after vascular injury (Heldin and Westermark, 1999). It has been reported that the anti-angiogenic activity of *G. lucidum* polysaccharides is achieved directly by inhibition of vascular endothelial cells proliferation. In the present study, we demonstrated that EORP reduced the proliferation (Fig. 1) and migration (Supplemental data, Figure I), not the de-differentiation (Supplemental data, Figure II) of PDGF-treated HASMCs in the *in vitro* study. Furthermore, an effect of EORP was also observed in vivo, as oral administration of EORP significantly reduced both cell proliferation and neointimal formation in a murine model of wire-induced vascular injury. Since SMC proliferation is a major characteristic of the neointima, our findings suggest an additional mechanism by which EORP treatment may be important in preventing the progression of cardiovascular disorders. The previous study demonstrated that *Ganoderma lucidum* extract attenuates the proliferation of hepatic stellate cells by blocking the PDGF receptor (Wang et al., 2009). The effects of EORP on PDGF levels in serum as well as PDGF receptor expression both in histological sections and in vitro cultured HASMCs will need further investigation.

In summary, this study provides the first evidence that EORP reduces the proliferation of PDGF-treated HASMCs *in vitro* and cell proliferation in the neointima and the neointima/media area ratio in the endothelial-denuded artery in mice *in vivo*. The present data suggest that these effects might be caused by arrest of cell cycle progression, due to reduced levels of cyclin D1/CDK4 and cyclin E/CDK2 as a result of upregulation of $p27^{Kip1}$ expression and inhibition of JNK phosphorylation. Since the proliferation of SMCs in the intima is a crucial step in the pathogenesis of

vascular diseases, our results imply that EORP may have therapeutic potential in the prevention of cardiovascular disorders, with beneficial effects in multiple pathological events involving cell proliferation, including inflammation and vascular diseases.

Acknowledgments

This work was supported by research grants from the National Science Council (NSC 99-2320-B-002-022-MY3) and the Cooperative Research Program of the NTU and CMUCM (100F008-404), Taiwan, Republic of China.

Literature Cited

Andres V, Castro C. 2003. Antiproliferative strategies for the treatment of vascular proliferative disease. Curr Vasc Pharmacol 1:85-98.

Desbois-Mouthon C, Cadoret A, Blivet-Van Eggelpoel MJ, Bertrand F, Caron M, Atfi A, Cherqui G, Capeau J. 2000. Insulin-mediated cell proliferation and survival involve inhibition of c-Jun N-terminal kinases through a phosphatidylinositol 3-kinase- and mitogen-activated protein kinase phosphatase-1-dependent pathway. Endocrinology 141:922-931.

Dudhgaonkar S, Thyagarajan A, Sliva D. 2009. Suppression of the inflammatory response by triterpenes isolated from the mushroom *Ganoderma lucidum*. Int Immunopharmacol 9:1272-1280.

Dzau VJ, Braun-Dullaeus RC, Sedding DG. 2002. Vascular proliferation and atherosclerosis: new perspectives and therapeutic strategies. Nat Med 8:1249-1256.

Evans S, Dizeyi N, Abrahamsson PA, Persson J. 2009. The effect of a novel botanical agent TBS-101 on invasive prostate cancer in animal models. Anticancer Res 29:3917-3924.

Gao Y, Gao H, Chan E, Tang W, Xu A, Yang H, Huang M, Lan J, Li X, Duan W, Xu C, Zhou S. 2005. Antitumor activity and underlying mechanisms of ganopoly, the refined polysaccharides extracted from *Ganoderma lucidum*, in mice. Immunol Invest 34:171-198.

Ghosh SS, Gehr TW, Ghosh S, Fakhry I, Sica DA, Lyall V, Schoolwerth AC. 2003. PPARgamma ligand attenuates PDGF-induced mesangial cell proliferation: role of MAP kinase. Kidney Int 64:52-62.

Golias CH, Charalabopoulos A, Charalabopoulos K. 2004. Cell proliferation and cell cycle control: a mini review. Int J Clin Pract 58:1134-1141.

Heldin CH, Westermark B. 1999. Mechanism of action and in vivo role of platelet-derived growth factor. Physiol Rev 79:1283-1316.

Hsu HY, Hua KF, Lin CC, Lin CH, Hsu J, Wong CH. 2004. Extract of Reishi polysaccharides induces cytokine expression via TLR4-modulated protein kinase signaling pathways. J Immunol 173:5989-5999.

Ishizawa K, Izawa-Ishizawa Y, Ohnishi S, Motobayashi Y, Kawazoe K, Hamano S, Tsuchiya K, Tomita S, Minakuchi K, Tamaki T. 2009. Quercetin glucuronide inhibits cell migration and proliferation by platelet-derived growth factor in vascular smooth muscle cells. J Pharmacol Sci 109:257-264.

Jiang J, Slivova V, Harvey K, Valachovicova T, Sliva D. 2004. *Ganoderma lucidum* suppresses growth of breast cancer cells through the inhibition of Akt/NF-kappaB signaling. Nutr Cancer 49:209-216.

Jiang J, Slivova V, Sliva D. 2006. *Ganoderma lucidum* inhibits proliferation of human breast cancer cells by down-regulation of estrogen receptor and NF-kappaB signaling. Int J Oncol 29:695-703.

Kim HS, Cho HJ, Park SJ, Park KW, Chae IH, Oh BH, Park YB, Lee MM. 2004. The essential role

of p21 in radiation-induced cell cycle arrest of vascular smooth muscle cell. J Mol Cell Cardiol 37:871-880.

Lin CY, Chen YH, Hsu HY, Wang SH, Liang CJ, Kuan, II, Wu PJ, Pai PY, Wu CC, Chen YL. 2010. *Ganoderma lucidum* polysaccharides attenuate endotoxin-induced intercellular cell adhesion molecule-1 expression in cultured smooth muscle cells and in the neointima in mice. J Agric Food Chem 58:9563-9571.

Lin SJ, Shyue SK, Hung YY, Chen YH, Ku HH, Chen JW, Tam KB, Chen YL. 2005. Superoxide dismutase inhibits the expression of vascular cell adhesion molecule-1 and intracellular cell adhesion molecule-1 induced by tumor necrosis factor-alpha in human endothelial cells through the JNK/p38 pathways. Arterioscler Thromb Vasc Biol 25:334-340.

Miyazaki T, Nishijima M. 1981. Studies on fungal polysaccharides. XXVII. Structural examination of a water-soluble, antitumor polysaccharide of *Ganoderma lucidum*. Chem Pharm Bull 29:3611-3616.

Moon SK, Kim HM, Lee YC, Kim CH. 2004. Disialoganglioside (GD3) synthase gene expression suppresses vascular smooth muscle cell responses via the inhibition of ERK1/2 phosphorylation, cell cycle progression, and matrix metalloproteinase-9 expression. J Biol Chem 279:33063-33070.

Ross R. 1995. Cell biology of atherosclerosis. Annu Rev Physiol 57:791-804.

Sata M, Maejima Y, Adachi F, Fukino K, Saiura A, Sugiura S, Aoyagi T, Imai Y, Kurihara H, Kimura K, Omata M, Makuuchi M, Hirata Y, Nagai R. 2000. A mouse model of vascular injury that induces rapid onset of medial cell apoptosis followed by reproducible neointimal hyperplasia. J Mol Cell Cardiol 32:2097-2104.

Shankland SJ, Wolf G. 2000. Cell cycle regulatory proteins in renal disease: role in hypertrophy, proliferation, and apoptosis. Am J Physiol Renal Physiol 278:F515-529.

Shiao MS. 2003. Natural products of the medicinal fungus *Ganoderma lucidum*: occurrence, biological activities, and pharmacological functions. Chem Rec 3:172-180.

Sliva D, Labarrere C, Slivova V, Sedlak M, Lloyd FP, Jr., Ho NW. 2002. *Ganoderma lucidum* suppresses motility of highly invasive breast and prostate cancer cells. Biochem Biophys Res Commun 298:603-612.

Sun J, He H, Xie BJ. 2004. Novel antioxidant peptides from fermented mushroom *Ganoderma lucidum*. J Agric Food Chem 52:6646-6652.

Thyagarajan A, Jiang J, Hopf A, Adamec J, Sliva D. 2006. Inhibition of oxidative stress-induced invasiveness of cancer cells by *Ganoderma lucidum* is mediated through the suppression of interleukin-8 secretion. Int J Mol Med 18:657-664.

Uchida K, Sasahara M, Morigami N, Hazama F, Kinoshita M. 1996. Expression of platelet-derived growth factor B-chain in neointimal smooth muscle cells of balloon injured rabbit femoral arteries. Atherosclerosis 124:9-23.

Wang GJ, Huang YJ, Chen DH, Lin YL. 2009. *Ganoderma lucidum* extract attenuates the proliferation of hepatic stellate cells by blocking the PDGF receptor. Phytother Res 23:833-839.

Wang SY, Hsu ML, Hsu HC, Tzeng CH, Lee SS, Shiao MS, Ho CK. 1997. The anti-tumor effect of *Ganoderma lucidum* is mediated by cytokines released from activated macrophages and T lymphocytes. Int J Cancer 70:699-705.

Wang YY, Khoo KH, Chen ST, Lin CC, Wong CH, Lin CH. 2002. Studies on the immuno-modulating and antitumor activities of *Ganoderma lucidum* (Reishi) polysaccharides: functional and proteomic analyses of a fucose-containing glycoprotein fraction responsible for the activities. Bioorg Med Chem 10:1057-1062.

Xie JT, Wang CZ, Wicks S, Yin JJ, Kong J, Li J, Li YC, Yuan CS. 2006. *Ganoderma lucidum* extract inhibits proliferation of SW 480 human colorectal cancer cells. Exp Oncol 28:25-29.

Zhan Y, Kim S, Izumi Y, Izumiya Y, Nakao T, Miyazaki H, Iwao H. 2003. Role of JNK, p38, and ERK in platelet-derived growth factor-induced vascular proliferation, migration, and gene expression. Arterioscler Thromb Vasc Biol 23:795-801.

Figure legends

Figure 1. EORP inhibits the proliferation of PDGF-treated HASMCs. HASMCs were incubated in serum-free medium in the presence of 0-10 μg/mL of EORP for 24 h, then were stimulated with 30 ng/mL of PDGF for 24 h, when cell viability, total cell number, and proliferation were evaluated by the MTT assay (A), cell counting (B), and staining for BrdU incorporation (C), respectively; the control (SF) was cells in serum-free medium not treated with EORP or PDGF. (D) Quantitative data for BrdU incorporation staining relative to the control value (no EORP and no PDGF). (E) Cell death was measured by LDH assay. (F) Cell apoptosis was examined by TUNEL assay. The data are the mean ± SEM for three independent experiments, each performed in triplicate. □ $P<0.05$ compared to the untreated control; † $P<0.05$ compared to PDGF alone.

Figure 2. EORP alters the expression of cell cycle regulatory proteins in PDGF-treated HASMCs. Cells were either left untreated or were treated for 24 h with EORP, then incubated with or without 30 ng/mL of PDGF for 24 h, then equal amounts of cell lysate proteins were subjected to SDS-PAGE followed by Western blot analysis using antibodies against cyclin D1 (A), CDK4 (B), cyclin E (C), CDK2 (D), $p27^{Kip1}$ (E), or $p21^{Cip1}$ (F) as described in the Materials and Methods. β-actin or α-tubulin was processed in parallel as an internal control for protein loading and the staining for the test protein band normalized to that of the β-actin or α-tubulin band. The results are shown as the fold increase in expression relative to that in untreated controls. The data are the mean ± SEM ($n = 3$). □ $P < 0.05$ compared to untreated controls, † $P < 0.05$ compared to

PDGF-treated cells.

Figure 3. Effect of EORP expression on the phosphorylation of MAPKs and Akt in PDGF-treated HASMCs. Cells were treated for 24 h with 10 μg/mL of EORP, then were incubated with or without 30 ng/mL of PDGF for 15 or 30 min, when equal amounts of cell lysate proteins were subjected to immunoblotting using antibodies against phosphorylated (upper panel) or total (lower panel) JNK (A), p38 (B), or ERK1/2 (C), or against p-Akt (D) or MKP-1 (E); the histograms show the phosphorylated band/total band intensity ratio for A-C and the p-Akt/GAPDH ratio for D or the MKP-1/α-tubulin ratio for E. $^{\square}P < 0.05$ compared to the untreated control, $^{\dagger}P < 0.05$ compared to PDGF-treated cells.

Figure 4. EORP prevents PDGF-induced HASMC proliferation by interfering with JNK signaling. HASMCs were incubated in serum-free medium in the presence or absence of 10 μg/mL of EORP for 18 h, then with different MAPK inhibitors for 6 h, and were stimulated with 30 ng/mL of PDGF for 24 h. The effect of EORP and MAPK inhibitors on the proliferation of PDGF-treated HASMCs was measured by BrdU incorporation staining (A) and the BrdU incorporation ratio (B). In B, the values are the mean ± SEM (n=3). $^{\square}P < 0.05$ compared to the untreated control, $^{\dagger}P < 0.05$ compared to PDGF-treated cells, $^{\ddagger}P < 0.05$ compared to PDGF+EORP-treated cells, $^{\S}P < 0.05$ compared to PDGF+PD- or PDGF+SB-treated cells.

Figure 5. Effects of MAPK inhibitors and EORP treatment on the expression of cyclin D1 (A), CDK4 (B), cyclin E (C), CDK2 (D), $p27^{Kip1}$ (E), or $p21^{Cip1}$ (F). HASMCs were incubated in serum-free medium in the presence or absence of 10 μg/mL of EORP for 18 h, then with different MAPK inhibitors for 6 h, and were stimulated with 30 ng/mL of PDGF for 24 h. The data presented are representative of three separate experiments. The values are the mean ± SEM (n=3). $^{\square}P < 0.05$ compared to the untreated control, $^{\dagger}P < 0.05$ compared to PDGF-treated cells, $^{\ddagger}P < 0.05$ compared to PDGF+SP- or PDGF+PD- or PDGF+SB-treated cells.

Figure 6. Effects of the transfection of HASMCs with JNK-specific siRNA on the expression of cyclin D1 (A), CDK4 (B), cyclin E (C), CDK2 (D), $p27^{Kip1}$ (E), or $p21^{Cip1}$ (F). (G) JNK-specific siRNA reduced JNK protein expression compared with non-treated cells. The PDGF-induced the increased CDK4, cyclinE, CDK2, and $p21^{Cip1}$ expression was inhibited by the transfection of HASMCs with JNK-specific siRNA. $^{\square}P < 0.05$ compared to the untreated control, $^{\dagger}P < 0.05$ compared to PDGF-treated cells, $^{\ddagger}P < 0.05$ compared to PDGF+EORP-treated cells.

Figure 7. EORP prevents neointima formation and cell proliferation *in vivo*. (A) Representative cross-sections of injured femoral arteries from mice fed a control diet (left) or a diet containing EORP (right) for 2 weeks stained with Resourcin-Fuchsin showing the internal elastic membrane (lower arrow). The neointima was indicated between two arrows. (B) Quantification of the neointima/media (I/M) ratio. (C) Immunohistochemical staining for PCNA (left panels) and smooth muscle cells (right panels) in serial sections of the femoral artery. Some PCNA-positive cells were

reacted with smooth muscle cell marker α-actin antibodies (arrowheads). (D) Percentage of proliferating cells (PCNA-positive) cells determined by dividing the number of PCNA-positive cells (brown color, arrowheads in Fig. 7C) by the total cell number per section. In B and D, the values are the mean ± SEM (n=12). $^{*}P<0.05$ compared to the non-EORP-treated control. (E) Immnunohistochemical staining for ICAM-1 expression. Bar=50 μm.

Table 1. EORP inhibits the proliferation of PDGF-treated HASMCs by causing cell-cycle arrest at G0/G1 phase. Cells were left untreated or were treated for 24 h with 1, 5, or 10 μg/mL of EORP, then with 30 ng /mL of PDGF for 24 h; the control was cells in serum-free medium not treated with EORP or PDGF. The cells were harvested using trypsin, fixed with ethanol, and treated with RNAase, then DNA was stained using propidium iodide and the percentage of cells in G0/G1 phase, S phase, or G2/M phase determined by FACScan profile analysis.

Table 1. EORP inhibits the proliferation of PDGF-treated HASMCs by causing cell-cycle arrest at G0/G1 phase

	G0/G1	S	G2/M
serum free	89.2 ± 0.5	2.0 ± 0.3	8.9 ± 0.6
PDGF	81.6 ± 1.2*	5.5 ± 0.7*	13.0 ± 0.8*
PDGF + EORP (1 μg/mL)	82.6 ± 0.8	5.2 ± 0.6	12.1 ± 0.9
PDGF + EORP (5 μg/mL)	84.3 ± 0.6†	5.3 ± 0.7	10.5 ± 0.4†
PDGF + EORP (10 μg/mL)	86.0 ± 0.9†	3.5 ± 0.6†	10.6 ± 0.6†
EORP (10 μg/mL)	89.7 ± 0.5	1.8 ± 0.1	8.5 ± 0.3

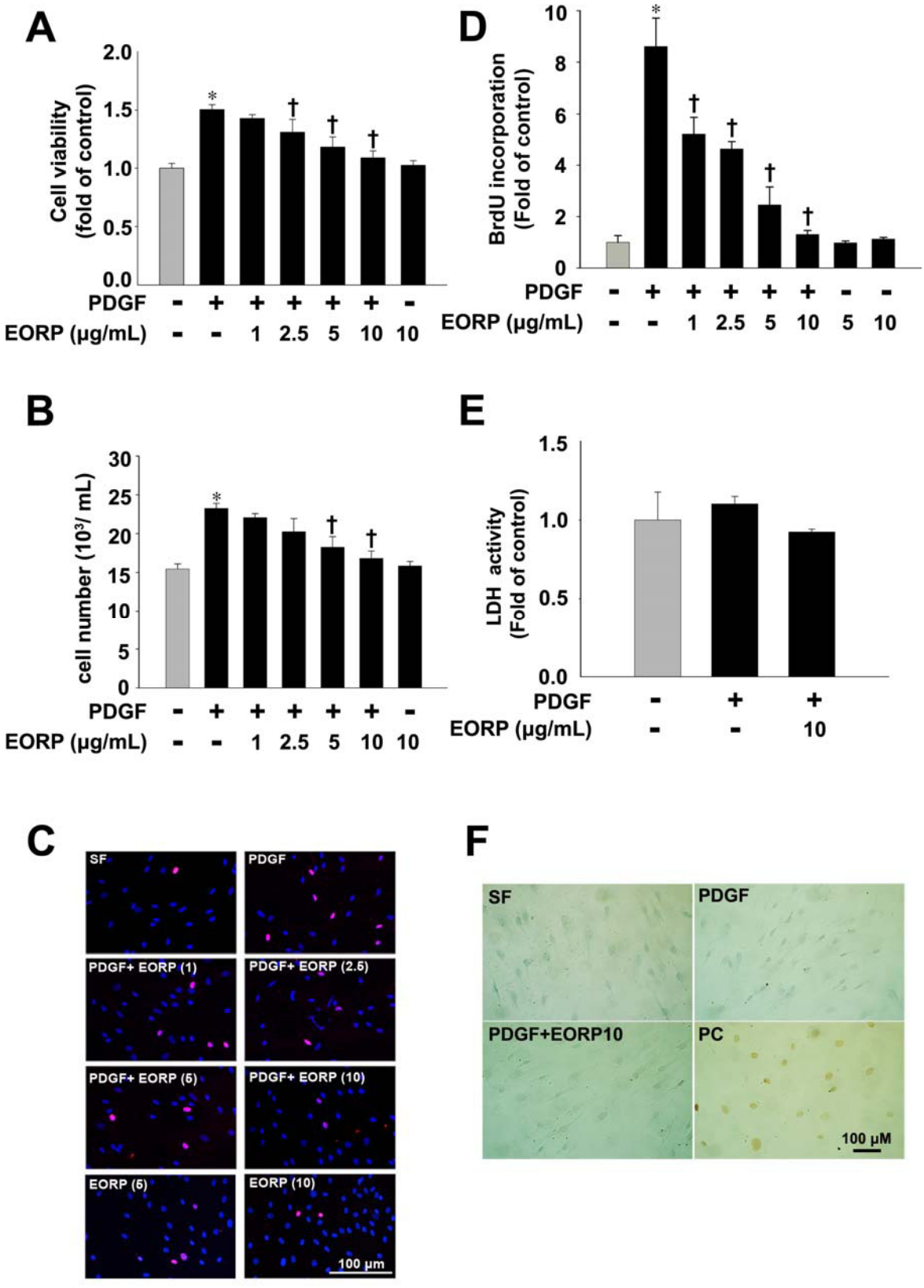

Fig. 1

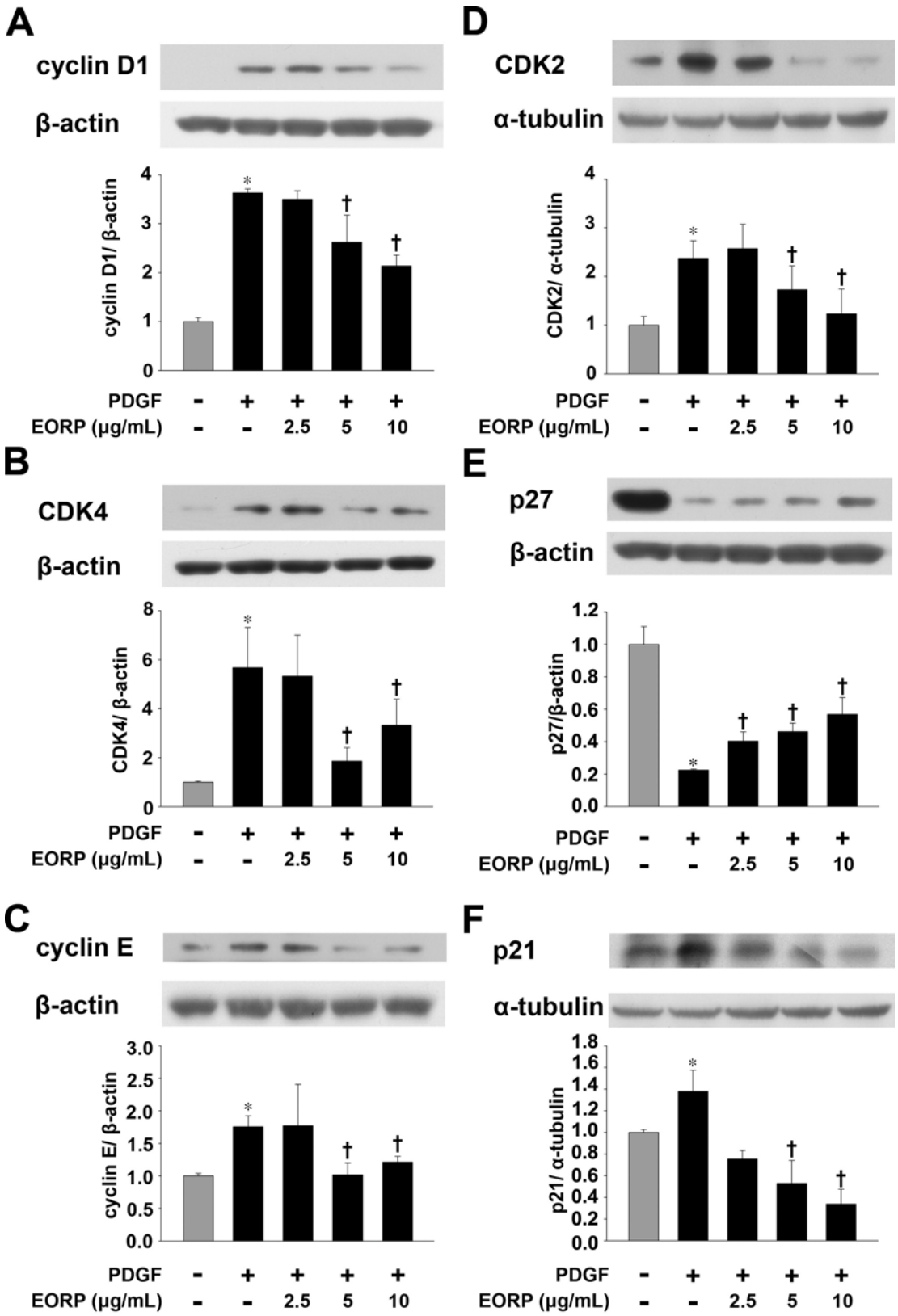

Fig. 2

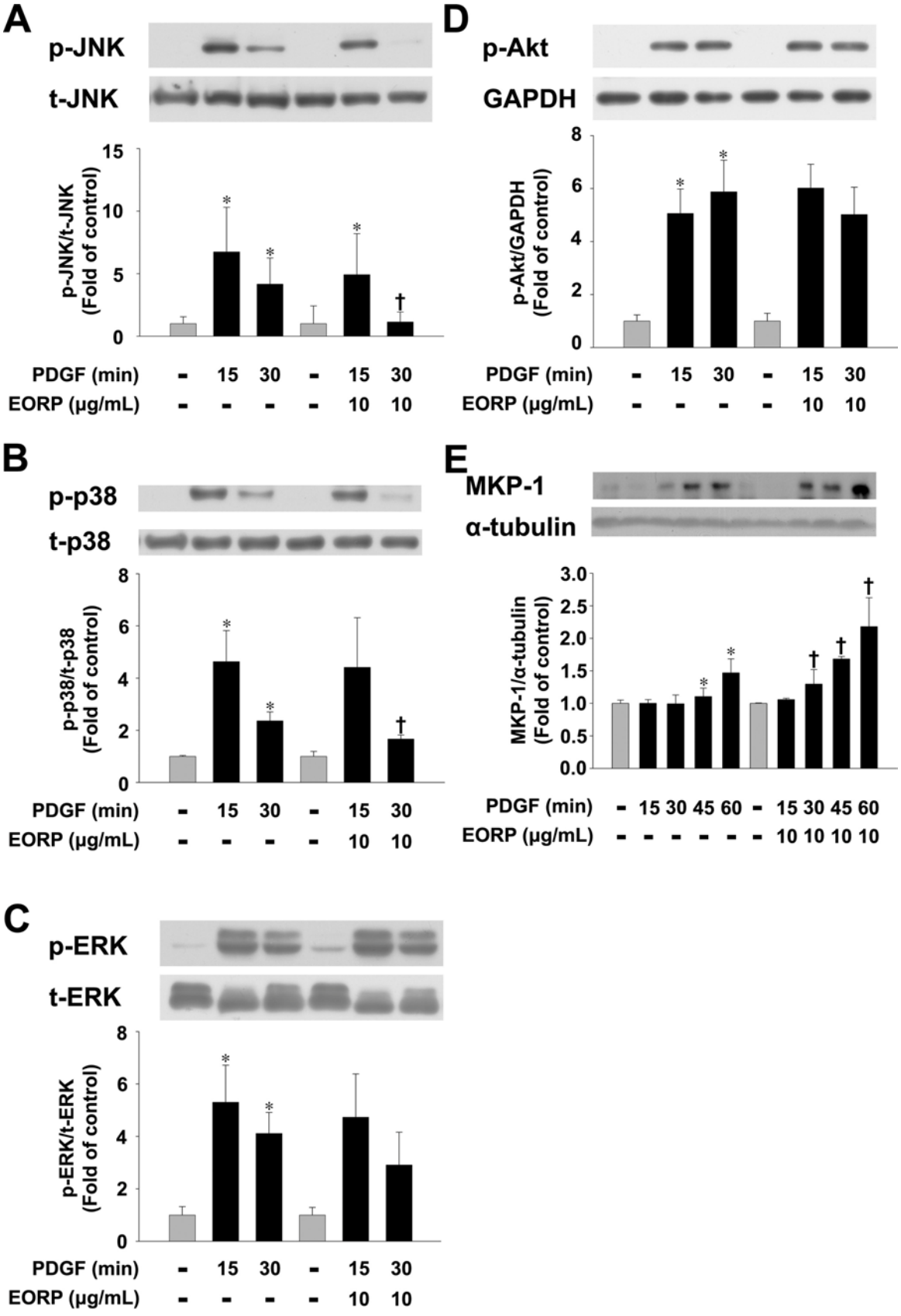

Fig. 3

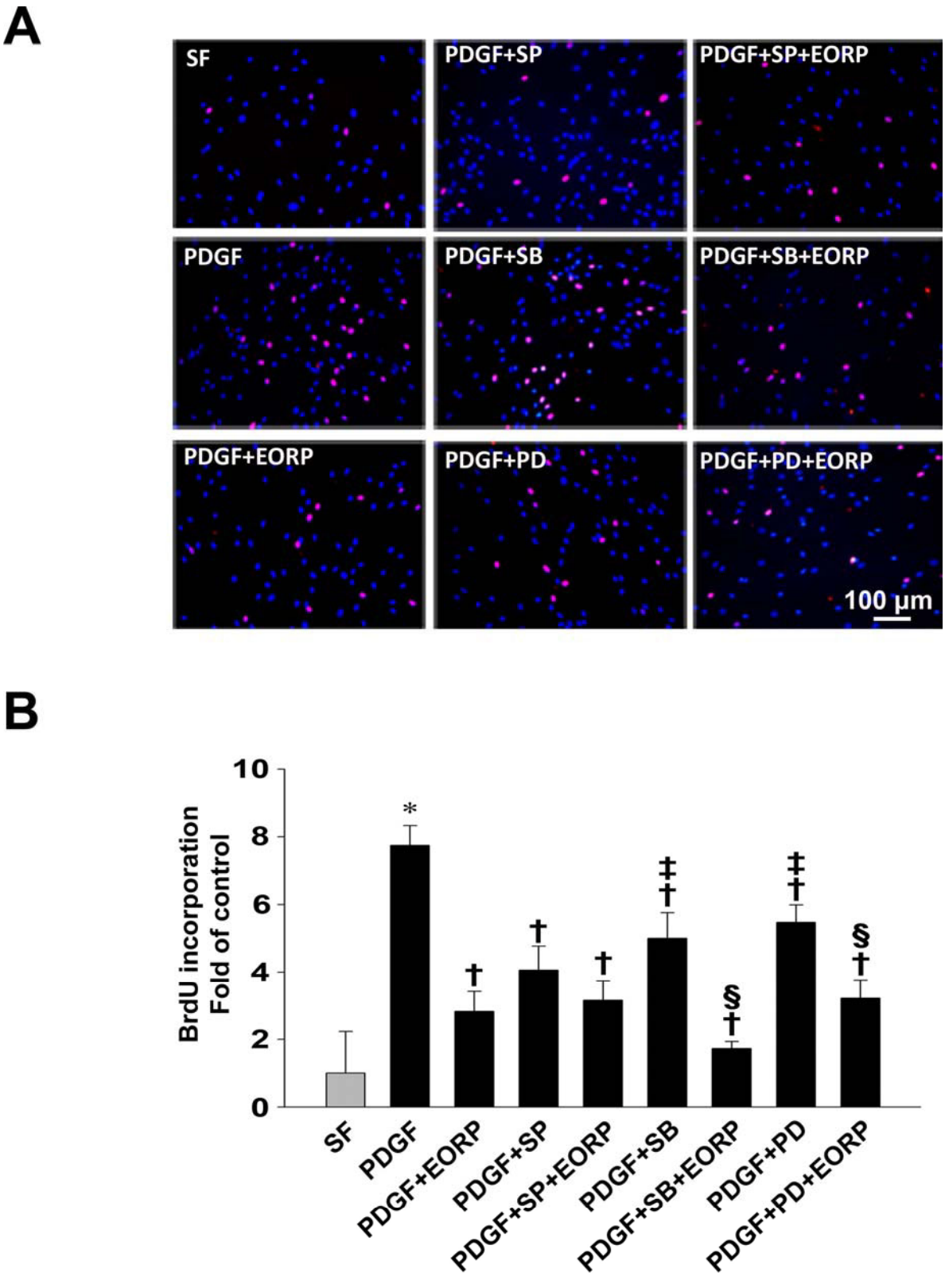

Fig. 4

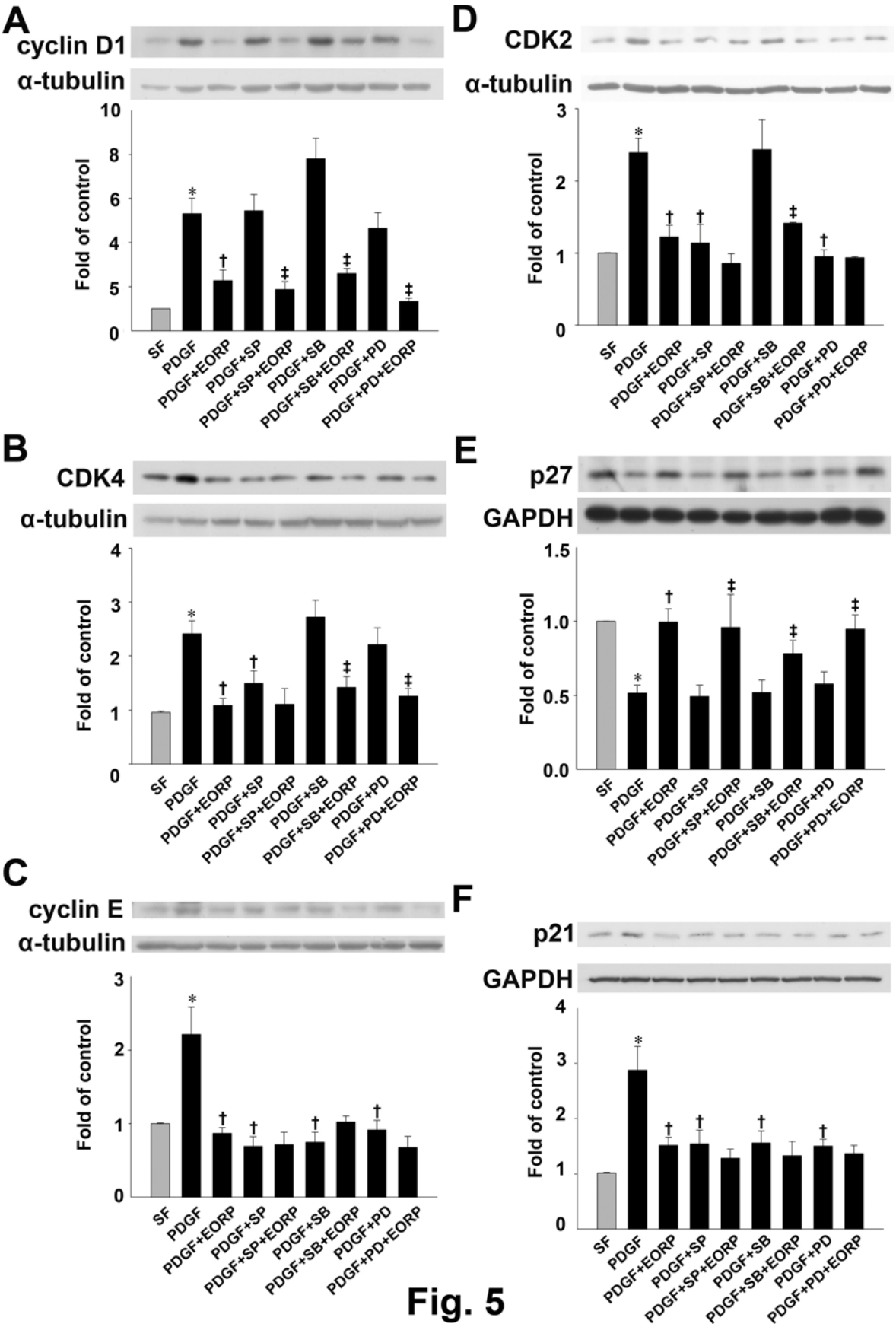

Fig. 5

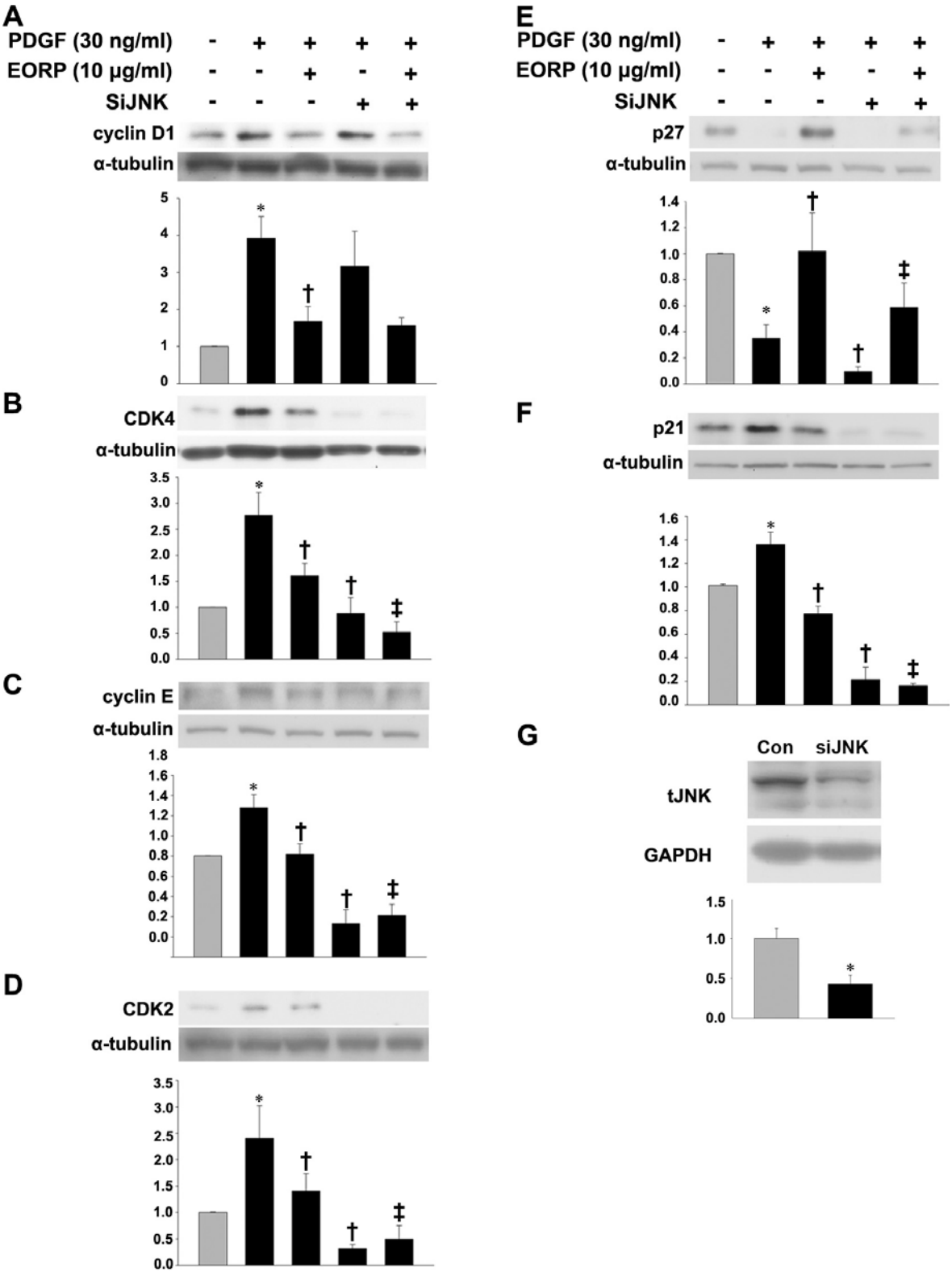

Fig. 6

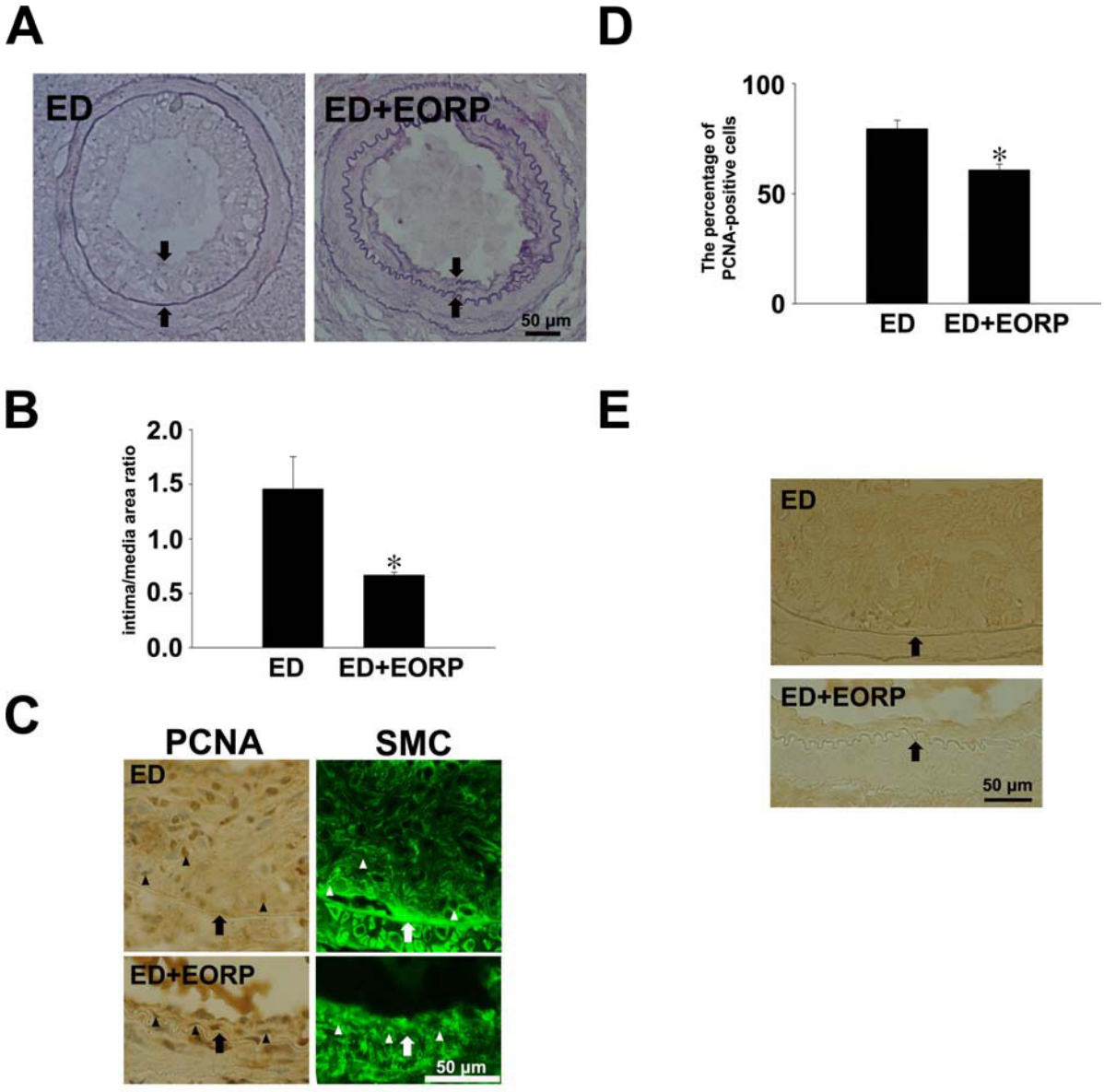

Fig. 7